

## RESEARCH ARTICLE

WILEY

# MozzieNet: A deep learning approach to efficiently detect malaria parasites in blood smear images

Sohaib Asif<sup>1</sup>  | Saif Ur Rehman Khan<sup>1</sup> | Xiaolong Zheng<sup>2</sup> | Ming Zhao<sup>1</sup>

<sup>1</sup>School of Computer Science and Engineering, Central South University, Changsha, China

<sup>2</sup>Department of Computer Science, Xi'an Research Institute of High Tech, Xi'an, China

## Correspondence

Sohaib Asif, School of Computer Science and Engineering, Central South University, Changsha, China.  
Email: [punjabians1592@gmail.com](mailto:punjabians1592@gmail.com)

## Abstract

Our study presents MozzieNet, a customized CNN model aimed at improving the identification of malaria parasites in blood smear microscopic images. By optimizing hyperparameters and incorporating techniques like data augmentation, batch normalization, and dropout, our model enhances robustness and generalization, addressing overfitting issues. Using the open-source NIH malaria dataset with 27,558 images, we achieve a classification accuracy of 96.73%, recall rate of 97.90%, precision of 95.67%, area under the curve (AUC) of 99.35%, and F1 score of 96.77%. We performed feature maps and Grad-CAM analysis on our proposed MozzieNet model to visualize and examine the targeted regions that are crucial for accurate predictions. Statistical analysis shows that the proposed architecture achieves promising performance and is superior to pre-trained models and existing methods for malaria detection. MozzieNet is designed for cloud and low-end smartphones, enabling malaria diagnosis in remote areas, thereby assisting physicians in informed malaria diagnosis and decision-making.

## KEYWORDS

computer-aided diagnosis, convolutional neural networks, deep learning, Grad-CAM, malaria detection, MozzieNet

## 1 | INTRODUCTION

Malaria is a parasitic illness that presents a significant worldwide health risk, with approximately 200 million individuals affected each year, and continues to be one of the most dangerous diseases on the planet.<sup>1</sup> Its history dates back to the 16th century B.C.<sup>2</sup> If malaria is not treated, it can lead to many complications, such as organ failure, anemia, hypoglycemia, respiratory distress, coma, and death. The disease usually spreads to humans through the female *Anopheles* mosquito. Several methods are available to detect *Plasmodium* in humans, including polymerization chain reaction (PCR),<sup>3</sup> rapid diagnostic test (RDT),<sup>4</sup> and microscopic examination of parasites in blood smears.<sup>5</sup> Malaria is mostly found in

underdeveloped regions of the world.<sup>6</sup> The gold standard for diagnosing this disease is microscopic observation of the parasite, as PCR and RDT are expensive. Microscopic analysis of blood smears for the detection of malaria parasites is a highly time-consuming and specialized process, requiring significant expertise to ensure accurate results. Each year, countless blood smear images are examined globally to identify malaria parasites. Examining a microscopic image of a blood smear involves several stages, such as collecting the sample, staining it, and then examining the slide to locate the infected cells. This technique is cumbersome, time-consuming, and complex, hence there is a need to come up with better solutions for the diagnosis of this disease. Thanks to recent advances in healthcare, if the carrier of a disease is correctly

diagnosed, then its spread can be prevented and it can be cured.

Computer-aided diagnosis (CADs) is very promising area in the field of artificial intelligence.<sup>31,32</sup> Therefore, in order to develop a successful CAD system, many researchers have investigated the principles of deep learning (DL) to detect malaria parasites to achieve superior accuracy.<sup>7,8</sup> For predictive models, DL methods require large amounts of medical data and high computational resources to learn different features. In the medical sector, access to labeled data is a problem due to the need for specialized expertise. In particular, the development of automated and accurate blood cell detection poses a special challenge for malaria detection and diagnosis. DL models, especially convolutional neural network (CNN), have proven very effective for variety of computer vision tasks because of its superior abilities to perform image analysis. DL models have the ability to process large datasets, which brings revolution in medical image analysis and therefore improves accuracy and efficiency. CNNs are widely used in biomedical imaging because it gives promising results in detection and classification of different disease.<sup>9,33,34</sup> DL models such as CNN can be very efficient, inexpensive, and scalable compared to deep pre-trained models. Deep models can provide maximum performance, but they have some drawbacks such as overfitting problems and a large number of layers making them computationally expensive and requiring longer training time. Weighted structure makes models computationally inexpensive by reducing parameters and complexity. CNNs can directly use images as the input of the network, include different layers such as convolution and max pooling for feature extraction, and have a high degree of undistorted deformation of images.

## 1.1 | Significance and novelty of this article

This study addresses a critical research gap in the field of malaria diagnosis by proposing a new DL model, MozzieNet, specifically designed for accurately classifying microscopic images of blood smears as infected or uninfected. Existing studies in the field have predominantly focused on deep models or transfer learning approaches, which may not be optimized for malaria detection and often come with heavy computational requirements. The research gap lies in the need for a specialized model that effectively addresses the challenges unique to malaria diagnosis. The complexity of malaria parasites and the variations in blood smear images require a tailored approach that can capture the subtle patterns indicative of infection. Previous methods may not adequately

account for these intricacies, leading to limitations in accuracy and robustness.

To fill this research gap, MozzieNet is developed with a customized architecture that integrates various layers, including convolution, pooling, and dense layers. Furthermore, techniques such as batch normalization, dropout, and LeakyReLU activation are incorporated to mitigate overfitting, accelerate training, and enhance the model's generalization ability specifically for malaria diagnosis. By developing MozzieNet and training it on a large dataset of 27 558 blood cell images, this study successfully addresses the research gap by providing a specialized DL model optimized for malaria detection. The impressive results achieved by MozzieNet demonstrate its potential to significantly improve the accuracy and efficiency of malaria diagnosis, thereby filling the existing research gap and contributing to the advancement of automated healthcare systems in combating this infectious disease. The main highlights of the proposed method are listed here:

- **Customized CNN Model (MozzieNet):** The paper proposes a novel DL model called MozzieNet, specifically designed for the identification of malaria parasites in blood smear microscopic images. MozzieNet is tailored to address the challenges associated with malaria diagnosis and leverages the power of CNNs for accurate classification.
- **Optimization of Hyperparameters:** The study focuses on optimizing the hyperparameters of the MozzieNet model, including image sizes, data augmentation techniques, optimizers, and batch size (BS). This optimization process ensures that MozzieNet achieves excellent performance, improved robustness, and enhanced generalization ability.
- **Integration of Techniques to Overcome Overfitting:** To overcome overfitting issues, the paper incorporates techniques such as batch normalization, dropout, and LeakyReLU activation. These techniques effectively mitigate overfitting problems and enable the MozzieNet model to achieve better convergence speed and improved classification performance.
- **Grad-CAM Analysis:** The paper utilizes Grad-CAM analysis, a visualization technique that provides color-coded representations of the regions in blood cell images that are crucial for accurate predictions. This approach enhances the interpretability of the MozzieNet model and provides valuable insights into the areas infected with malaria parasites.
- **Comparative Evaluation:** The performance of the MozzieNet model is rigorously evaluated and compared with pre-trained models and existing methods using various evaluation metrics. The results demonstrate

that MozzieNet surpasses the performance of pre-trained models and existing techniques, highlighting its superiority and effectiveness in malaria detection.

This paper is further divided into several sections, where Section 2 describes the literature review, and Section 3 describes our proposed model of work for the entire study. In Section 4, we presented experimental results and discussion of MozzieNet and comparison with current research, and the article concludes in Section 5.

## 2 | LITERATURE REVIEW

Recently, several efforts have been proposed to diagnose malaria using DL methods. Angel Molina et al.<sup>10</sup> proposed a DL model based on Vgg-16, which uses transfer learning technique to detect blood cells from malaria patients. The authors used 6415 images and achieved 99.5% accuracy, 100% sensitivity and 91.7% specificity. A. Vijayalakshmi et al.<sup>11</sup> proposed a DL model for malaria detection. They customized the architecture of the VGG-19 model, replacing the last layer with SVM, and achieved 93% accuracy in automatic detection of malaria. In Reference 12, the authors proposed a DL framework for segmentation of red blood cells and detection of malaria. They achieved 93.72% accuracy by segmentation on a test dataset. Jane Hung et al.<sup>13</sup> used a faster R-CNN model and applied fine-tuning. The authors compared the model with a baseline model including classification, segmentation, and feature extraction, and the results outperformed the baseline model. In Reference 14, it was found that support vector machines (SVMs) outperformed Bayes classifiers. Their study also found that combining these classifiers with majority voting techniques gives an accuracy of 96.5%, which is better than using only one of the classifiers. Rajaraman et al.<sup>15</sup> use five different transfer learned models (AlexNet, DenseNet-121, Resnet50, Xception, and vgg-16) and apply transfer learning technique for malaria parasite detection. They also proposed a custom CNN model using different layers and achieved 92.7% accuracy with the CNN model and 95.9% with the ResNet50 model. Gopakumar et al.<sup>16</sup> proposed a custom CNN and analyzed focal stacked images to find plasmodium parasite and compared it with the SVM model, and their study found that the custom CNN outperformed the SVM. Mehedi Masud et al.<sup>17</sup> have developed a custom CNN that uses the Cycling SGD Optimizer to classify healthy and infected cell images with 97.3% accuracy. They deployed the model in a mobile application to classify images of healthy and infected cells. Liang et al.<sup>18</sup> designed sequential CNN model containing 16 different

layers for malaria parasite detection. After rigorous experimentation, they concluded that their model was superior to other models. The detection of Plasmodium in thick blood smear images was addressed by Feng Yang<sup>19</sup> through the proposal of a DL model that utilized a specially designed CNN. The dataset contains 1890 images from 150 patients. They achieved excellent results on different evaluation matrices and deployed the proposed model in mobile devices for real-time detection of malaria parasites. Yasmin M. Kassim et al.<sup>20</sup> designed a novel technique for identifying and enumerating red blood cells in thin blood smear microscopic images. The architecture proposed by the authors consists of two different stages; the first stage is U-Net for cell cluster or segmentation and the second stage is Faster R-CNN for the detection of small objects. By using this model, they achieved an accuracy of 97%. Elter et al.<sup>21</sup> used feature extraction technique and classified the patient into infected and non-infected. They extracted 174 features from pre-detected malaria patients and obtained a sensitivity of 97% by applying support vector machines (SVM). Varma et al.<sup>22</sup> applied image processing techniques to count the exact number of parasites in plasmodia candidates. The authors proposed a local binary pattern technique to classify microscopy images of blood smears and compared the results using different evaluation matrices. Their system attained an accuracy of 88.3% and 83.5% when using thin and thick blood smear images, respectively.

## 3 | MATERIALS AND METHODS

This section provides a comprehensive overview of the MozzieNet model's architecture. It involves incorporating various layers such as multiple convolutional layers and the activation functions to accelerate convergence; drop-out layers are used after each dense layer to reduce overfitting and improve the generalization of the model. These components are used in different layers with activation functions to train our proposed MozzieNet model. Figure 1 shows the overall workflow approach of the study. We explain in detail the workflow methodology and various stages, such as the dataset description, data pre-processing and augmentation, the architecture of the proposed MozzieNet model, and hyperparameter tuning.

### 3.1 | Dataset used for experimentation

We used the publicly available malaria dataset from Reference 15 to evaluate our proposed model. The dataset was collected from healthy and malaria-infected patients

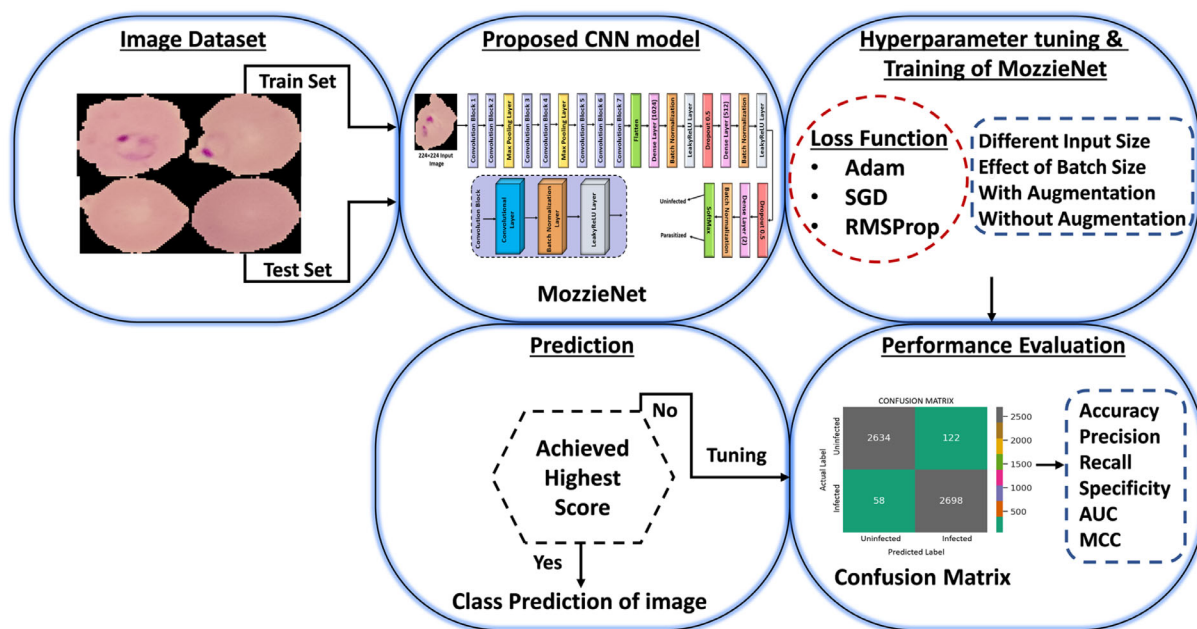


FIGURE 1 Workflow of our proposed MozzieNet model.

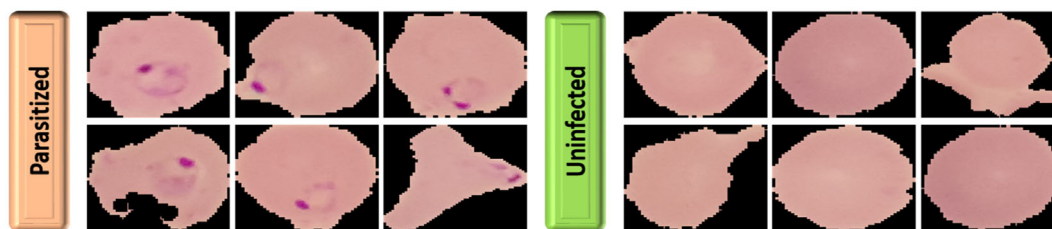


FIGURE 2 Sample of blood cell images from the dataset.

in medical hospitals in Bangladesh. The dataset was manually annotated by medical experts and subsequently approved by the National Library of Medicine. There are 27 558 images in each category with the same distribution of blood cell images, such as 13 779 images of parasites and uninfected patients, respectively. Uninfected cells do not contain Plasmodium, while parasitic cells contain Plasmodium and red globular structures. Figure 2 depicts blood cell samples from parasitic and uninfected class.

### 3.2 | Data pre-processing and augmentation

Data pre-processing is a necessary step in medical imaging. We use various pre-processing methods such as different image sizes  $25 \times 25 \times 3$ ,  $50 \times 50 \times 3$ , and  $100 \times 100 \times 3$  to evaluate the performance of MozzieNet on different input image sizes. The dataset containing 27 558 images was divided into three separate sets: a

TABLE 1 Splitting of malaria parasite dataset.

Set	Class		Percentage (%)
	Parasitized	Uninfected	
Training	9646	9645	70
Validation	1378	1378	10
Testing	2756	2756	20

training set, a validation set, and a test set. Table 1 shows the splitting of dataset.

Training models with insufficient data can cause overfitting issues. To overcome this, data augmentation techniques can be utilized to boost performance. In this study, we employed several data augmentation methods to enhance MozzieNet's capacity to adapt to diverse scenarios and mitigate overfitting issues. We have used ImageDataGenerator class provided by Keras for image augmentation. The images in training were augmented using different techniques: (1) horizontal flipping is applied, (2) images rotated by the angle of 20, (3) width



**TABLE 2** Parameters used for data augmentation.

Parameters	Value
Width_shift_range	0.1
Height_shift_range	0.1
Shear_range	0.1
Zoom_range	0.1
Horizontal_flip	True
Rotation_range	20
Fill_mode	Nearest

shift and height shift range of 0.1 are applied, (4) zoom range is 0.1, (5) shear range is 0.1, and (6) fill mode of nearest is applied. Table 2 presents the names and values of the parameters used in the current study to train our proposed MozzieNet model.

### 3.3 | MozzieNet architecture: Our proposed method for malaria diagnosis

DL-based methods are variants of machine learning (ML) algorithms that outperform conventional ML techniques. Due to their significant accuracy, DL-based models have shown impressive performance and have recently been applied in various fields, such as medical imaging, agriculture, and robotics. CNN has been specifically used for computer vision tasks to automatically extract and identify features of images. Due to its high performance, CNNs are becoming more and more popular in medical image classification problems.

This section describes the MozzieNet CNN model proposed for detecting malaria-infected patients. The general structure of the proposed MozzieNet CNN model is illustrated in Figure 3. The proposed CNN model consists of four separate blocks. The first two blocks contain four convolutional layers and two maximum pooling layers. In addition, the BN layer is sandwiched between each convolution layer and the activation function to speed up the training by reducing the complexity of the parameters. The third block contains three convolutional layers that use 256 filters of size  $3 \times 3$ , followed by a BN and activation function. The last block contains three dense layers, where the first two layers have 1024 and 512 neurons, the dropout rate of 0.5 is used to reduce overfitting, and the last layer has 2 neurons, using a Soft-max classifier to classify patients into infected and not infected.

Figure 4 depicts the layered architecture of the MozzieNet model. The first layer of the MozzieNet

architecture accepts pre-processed cell images with an input size of  $50 \times 50$ . The first and second blocks contain two convolutional layers for performing convolution operations with 64 convolutional filters and a kernel size of  $3 \times 3$ . Small kernel sizes in MozzieNet models can reduce training time compared to large kernel sizes, resulting in a large number of parameters. The BN layer is placed between the convolution layer and the activation function, increasing the stability of MozzieNet. The purpose of the BN layer is to achieve faster training, improve accuracy, and allow a higher learning rate. After the convolution process, the maximum pooling layer is used for non-overlapping sub-areas with a filter size of  $2 \times 2$  to achieve dimensionality reduction. This layer can reduce model parameters and minimize overfitting and storage space. The operation order of the third and fourth blocks is the same as that of the first two convolution blocks, with parametric differences. The convolution operation is performed on the first two layers of the third and fourth blocks using 128 filters of size  $3 \times 3$ . We equip each convolutional layer with a BN layer and then an LR. In general, ReLU is a commonly used activation function because it is simple. However, the negative side of ReLU activation is dead neurons. The dying ReLU refers to the problem when the units are not activated initially. This study uses LeakyReLU because it is a common effective method for solving the dying ReLU problem. Compared with other activation functions, the advantages of LR are well-known.<sup>23</sup> Leaky ReLU allows a slight slope for negative values, rather than a flat slope as shown in Equation (1).

$$f(x) = \begin{cases} 0.01x, & \text{for } x < 0 \\ x, & \text{for } x \geq 0 \end{cases} \quad (1)$$

LeakyReLU has two potential benefits:

1. Fixes “dying ReLU” issue and prevents the slope from becoming 0.
2. This can help prevent vanishing gradients and speed up training.

The last three convolution blocks contain three convolutional layers and use 256 filters of size  $3 \times 3$ . We used three BN layers in each convolutional layer, followed by the LR activation function. In addition to the convolution and pooling layers, our model used a flattening layer to flatten the entire model. Features retrieved from the last convolution block are flattened and transferred to the three dense layers.

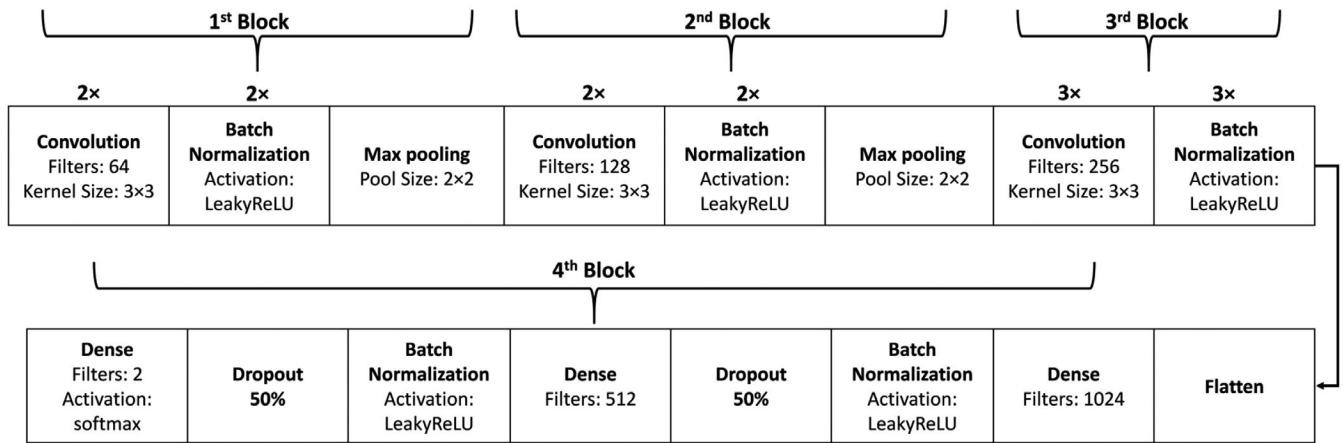


FIGURE 3 General architecture of the MozzieNet model.

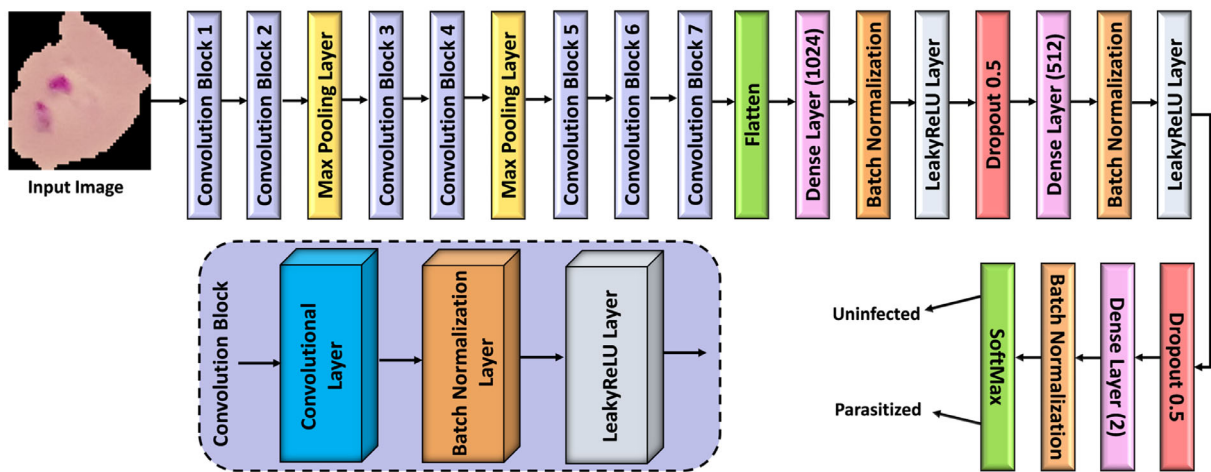


FIGURE 4 Proposed MozzieNet model for malaria parasite classification.

After the flattening layer, we use three dense layers to perform the classification task. The model's first and second dense layers comprise 1024 and 512 neurons, respectively, and implement LeakyReLU as their activation function. A BN layer is introduced between the activation function and the dense layers. Two dropout layers of 0.5 are used after each dense layer to avoid overfitting, and randomly drop out nodes to improve network generalization errors. The last dense layer contains two neurons and a Softmax activation function. A BN layer was added before the Softmax calculation to improve the final classification performance of the MozzieNet model. BN is a prevalent technique that enhances network stability and accelerates the training process. The output of this layer is the same as the number of classes. Table 3 details the layer types and their parameters used to train the proposed MozzieNet model. In this study, it is parasitized

and uninfected. The Softmax activation function is given as:

$$f(s)_i = \frac{e^{s_i}}{\sum_j e^{s_j}}, \quad (2)$$

where  $i$  represents the classes in the dataset and  $s$  in the input.

In order to provide a clear understanding of the MozzieNet model architecture, we have included pseudocode representation below. The pseudocode provides a step-by-step overview of the model's structure and the sequence of operations involved in the classification process. This representation serves as a valuable resource for better comprehending the inner workings of the MozzieNet model and its classification capabilities.

**TABLE 3** Architecture of the proposed MozzieNet model for malaria parasite classification.

Name	Layer (type)	Output shape	Parameters
Input	Input layer	$50 \times 50 \times 3$	0
Conv block 1	Convolution	$50 \times 50 \times 64$	1792
	BN and LR	$50 \times 50 \times 64$	256
Conv block 2	Convolution	$50 \times 50 \times 64$	36 928
	BN and LR	$50 \times 50 \times 64$	256
Max pooling	Pooling size = $(2 \times 2)$	$25 \times 25 \times 64$	0
Conv block 3	Convolution	$25 \times 25 \times 128$	73 856
	BN and LR	$25 \times 25 \times 128$	512
Conv block 4	Convolution	$25 \times 25 \times 128$	147 584
	BN and LR	$25 \times 25 \times 128$	512
Max pooling	Pooling size = $(2 \times 2)$	$12 \times 12 \times 128$	0
Conv block 5	Convolution	$12 \times 12 \times 256$	295 168
	BN and LR	$12 \times 12 \times 256$	1024
Conv block 6	Convolution	$12 \times 12 \times 256$	590 080
	BN and LR	$12 \times 12 \times 256$	1024
Conv block 7	Convolution	$12 \times 12 \times 256$	590 080
	BN and LR	$12 \times 12 \times 256$	1024
Flatten	Flatten	36 864	0
Fully connected 1	Dense (1024 neurons)	1024	37 749 760
	BN, LR	1024	4096
Dropout	Dropout (0.5)	1024	0
Fully connected 2	Dense (512 neurons)	512	524 800
	BN, LR	512	2048
Dropout	Dropout (0.5)	512	0
Fully Connected 3	Dense (2 neurons)	2	1024
	BN	2	8
	Softmax	2	0

Pseudocode: Input: Image data with shape (50, 50, 3)

# Convolutional Block 1

Conv1 = Convolutional Layer with 64 filters of size (3, 3), stride = 1

BN1 = Batch Normalization(Conv1)

LR1 = LeakyReLU(BN1)

# Convolutional Block 2

Conv2 = Convolutional Layer with 64 filters of size (3, 3), stride = 1

BN2 = Batch Normalization(Conv2)

LR2 = LeakyReLU(BN2)

# Max Pooling

MaxPool1 = Max Pooling layer with pool size (2, 2)

# Convolutional Block 3

Conv3 = Convolutional Layer with 128 filters of size (3, 3), stride = 1

BN3 = Batch Normalization(Conv3)

LR3 = LeakyReLU(BN3)

# Convolutional Block 4

Conv4 = Convolutional Layer with 128 filters of size (3, 3), stride = 1

BN4 = Batch Normalization(Conv4)

LR4 = LeakyReLU(BN4)

# Max Pooling

MaxPool2 = Max Pooling layer with pool size (2, 2)

# Convolutional Block 5

Conv5 = Convolutional Layer with 256 filters of size (3, 3), stride = 1

BN5 = Batch Normalization(Conv5)

LR5 = LeakyReLU(BN5)

# Convolutional Block 6

(Continues)

(Continues)

Conv6 = Convolutional Layer with 256 filters of size (3, 3),  
stride = 1

BN6 = Batch Normalization(Conv6)

LR6 = LeakyReLU(BN6)

# Convolutional Block 7

Conv7 = Convolutional Layer with 256 filters of size (3, 3),  
stride = 1

BN7 = Batch Normalization(Conv7)

LR7 = LeakyReLU(BN7)

# Flatten

Flatten1 = Flatten Layer()

# Fully Connected Layer 1

FC1 = Fully Connected Layer with 1024 neurons

BN\_FC1 = Batch Normalization(FC1)

LR\_FC1 = LeakyReLU(BN\_FC1)

# Dropout

Dropout1 = Dropout Layer(rate = 0.5)

# Fully Connected Layer 2

FC2 = Fully Connected Layer with 512 neurons

BN\_FC2 = Batch Normalization(FC2)

LR\_FC2 = LeakyReLU(BN\_FC2)

# Dropout

Dropout2 = Dropout Layer(rate = 0.5)

# Fully Connected Layer 3

FC3 = Fully Connected Layer with 2 neurons (output layer)

BN\_FC3 = Batch Normalization(FC3)

Output = Softmax(BN\_FC3)

# Model Compilation

Compile the model with appropriate optimizer, loss function,  
and evaluation metrics

# Model Training

Train the model on the training dataset with specified batch  
size and number of epochs

# Model Evaluation

Evaluate the model on the test dataset

### 3.4 | Hyperparameters tuning and optimization

The primary objective of this task is to introduce a CNN model that is both robust and highly efficient in categorizing parasites and uninfected blood smears, with the aim of diagnosing malaria. The optimal configuration of hyperparameters plays a crucial role in achieving the best accuracy. To optimize the proposed MozzieNet model, several experiments are performed in which

various hyperparameter values are tested until the best model is reached. We trained our proposed MozzieNet model using microscopic images of blood smears to classify malaria parasites. Data shuffling was performed on the training data before each epoch. The learning rate (LR) of 0.001 is used for training the MozzieNet model and is also one of the important hyperparameters. Four different BSs were used to evaluate its impact on test accuracy as it is the most critical hyperparameter for best-generalized performance. The minimum BS is set to 16. The input image size is a key hyperparameter that affects the performance of the model. Small-size images are memory efficient and take less time. On the other hand, the larger the image, the more computational resources are needed to learn all the parameters. In our data collection, due to the different original image sizes, we evaluated different input image sizes and observed that the image size of  $50 \times 50$  provides higher performance. Table 4 exhibits the hyperparameters of the MozzieNet architecture and their corresponding values.

To avoid overfitting in our work, we used 50% dropout and the image data are augmented using a data augmentation technique. We train a MozzieNet model using an early stopping method that controls the number of epochs; this method stops training as soon as the performance of the model stops improving on the validation dataset. We added a BN layer before each LeakyReLU activation function to regularize the model and reduce the need for dropout. A BN layer is added before the activation functions to improve the performance of the MozzieNet model. BN flattens the optimization problems, taking advantage of the significantly higher

**TABLE 4** Hyperparameters and the values of the proposed MozzieNet model.

Parameters	Value
LR	0.001
BS	16, 32, 64, 128
Epochs	20, 50, 100
Loss Function	Categorical Cross-entropy
Activation	LeakyReLU in convolutional layers Softmax in final fully connected layer
Optimizers	Adam, RMSProp, SGD
Shuffle	Every-epoch
Dropout rate	50%
Pooling	Max $2 \times 2$
Input Shape	$25 \times 25$ , $50 \times 50$ , $100 \times 100$



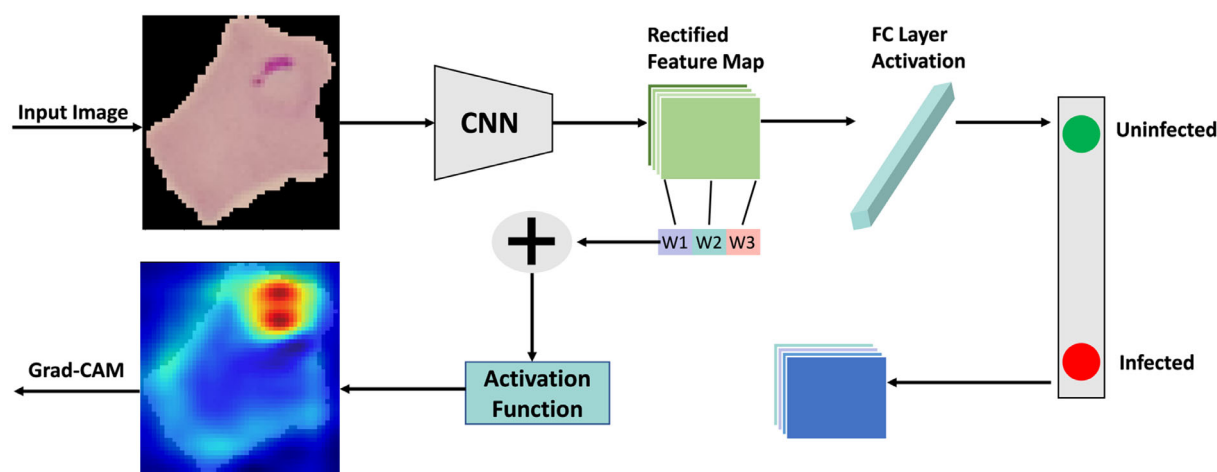


FIGURE 5 Simple explanatory diagram to describe the Grad-CAM method.

learning rate and more stable training of the dataset with MozzieNet.

### 3.5 | Grad-CAM

Numerous efforts have been made in different DL applications involving medical imaging to enhance the interpretability of the results. Selvaraju et al.<sup>24</sup> proposed a Grad-CAM method that provides an explainable visualization of DL models. It provides a visual interpretation of the model and helps to determine more information when performing detection. As shown in Figure 5, the Grad-CAM algorithm is applied to our MozzieNet model to determine the transparency of malaria parasite detection. Grad-CAM is applied to any convolutional layer while using the complete model to calculate the predicted label. In most cases, the last convolution layer is used to apply the Grad-CAM.

## 4 | RESULTS AND DISCUSSION

In this section, we discuss the performance analysis and results of our MozzieNet model obtained from several experiments using different key metrics. In this article, the aim is to classify microscopic blood images. The classification of parasitic and uninfected images requires several steps from pre-processing to recognition. Most of the previous models analyzed their effectiveness using the publicly available malaria dataset published by Reference 15. Therefore, we also considered the same dataset for performance evaluation and compared the results obtained by MozzieNet model with the existing methods.

TABLE 5 Performance evaluation metrics.

Performance metric	Mathematical equation
Accuracy (ACC)	$\frac{trp + trn}{trp + trn + fan + fap}$
Matthews correlation coefficient (MCC)	$\frac{(trp \times trn - fan \times fan)}{\sqrt{(trp + fan)(trp + fan)(trn + fan)(trn + fan)}}$
Precision (PRE)	$\frac{trp}{trp + fan}$
Specificity (SPEC)	$\frac{trn}{trn + fap}$
F1 score (F1)	$2 \times \frac{Precision \times Recall}{Precision + Recall}$
Recall (REC)	$\frac{trp}{trp + fan}$

### 4.1 | Experimental setup

We have implemented the MozzieNet model using Python with Tensorflow, Keras, and Scikit Learn for training and reporting classification performance. The designed model has been validated with the operating system Window 7 64-bit and training is done using an Nvidia K80 Tesla GPU provided by Google Colab, 16 GB RAM, and 128 GB of disk space.

### 4.2 | Evaluation metrics

The classification results of the proposed MozzieNet model are evaluated using various performance metrics shown in Table 5. Where trp and trn denote true positive and true negative, and fan and fap denote false negative and false positive. Sensitivity measures the percentage of infected images predicted by MozzieNet. Precision is the reliability of the model in classifying parasitic images. The confusion matrix is the most commonly used metric

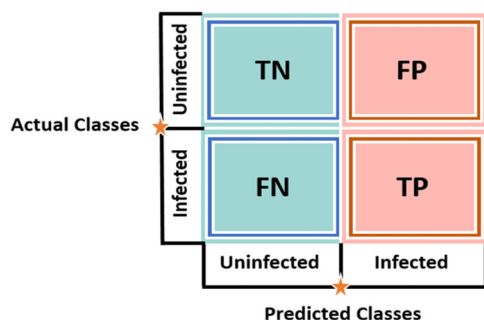


FIGURE 6 Confusion matrix.

specifically used for classification problems. In short, the confusion matrix visualizes the performance of the model with detailed information about the correct and incorrect classifications. Figure 6 displays the confusion matrix for the binary classification task.

### 4.3 | Performance evaluation

This section presents performance analysis of MozzieNet models using various performance metrics. A total of 19 290 and 2756 images are used to train and validate the MozzieNet model. During the testing, 5512 images were used. Since the proposed MozzieNet architecture requires multiple parameters, choosing the right hyperparameters allows for faster convergence. The model underwent 100 epochs during the training process, with a BS of 64. The input images were resized to  $50 \times 50$  pixel dimensions. The presented results in Table 6 outline the performance of our MozzieNet model using various performance metrics. The overall accuracy of the MozzieNet model was found to be the highest at 96.73%, with a recall of 97.90% and an F1 score of 96.77%.

We also reported MozzieNet class-wise results on the test set by calculating precision, recall, and F1 scores for each class to obtain overall performance. The MozzieNet model achieved a classification score of over 95% for predicting both classes. The class-wise results of the model are tabulated in Table 7, indicating a well-balanced F1 score of approximately 97%. It is noteworthy that the model achieved a recall rate of 98% for the infected class.

Figures 7 and 8 illustrate the learning curves of the MozzieNet model over 100 epochs concerning training and validation accuracy, as well as the model loss during training and validation. The figures demonstrate that the proposed MozzieNet model is appropriately trained, indicating that the model is neither underfitting nor overfitting. Furthermore, the developed model achieved the highest accuracy while exhibiting the lowest loss. A

TABLE 6 Performance statistics of the proposed MozzieNet model.

Performance metric	Proposed MozzieNet scores (%)
ACC	96.73
REC	97.90
PRE	95.67
SPEC	95.57
F1	96.77
MCC	93.49
AUC	99.35

TABLE 7 Class-wise precision, recall, and F1 score of MozzieNet model.

Class	PRE	REC	F1
Uninfected	0.98	0.96	0.97
Infected	0.96	0.98	0.97
Macro average	0.97	0.97	0.97
Weighted average	0.97	0.97	0.97
Overall accuracy of the MozzieNet model	96.73%		

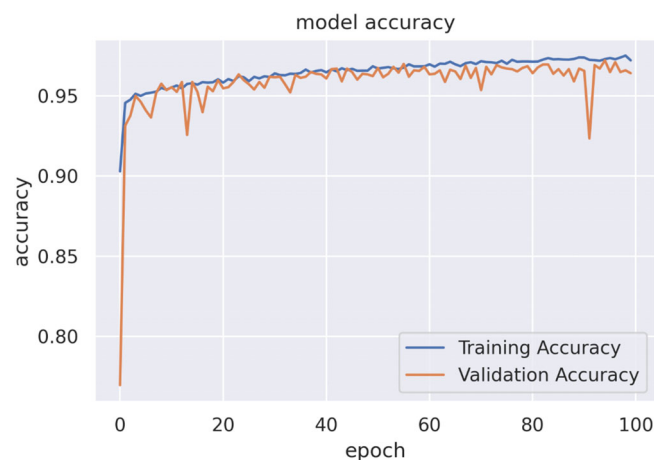


FIGURE 7 Training and validation learning curves of the MozzieNet model.

significant reduction in verification loss was detected at the beginning of the training process.

- We add a BN layer before each activation function to improve the final classification accuracy because the BN layer is usually placed before the activation function.
- Use of “LeakyReLU” as an activation function to fix the dying ReLU problem and “Adam” as an optimizer for very high computational efficiency.

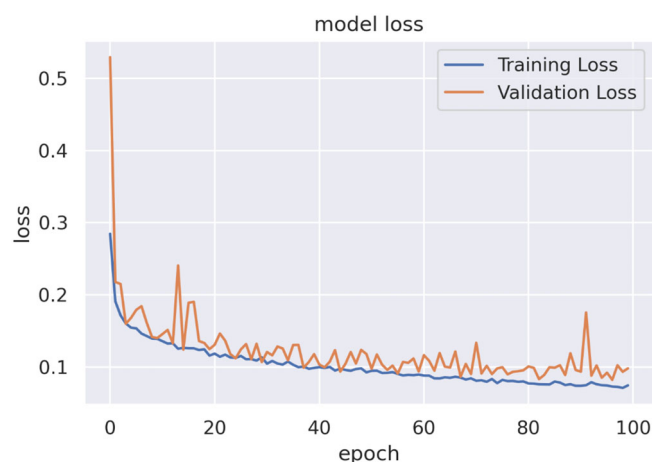


FIGURE 8 Loss curves of the MozzieNet model.

- Data augmentation is used to reduce the risk of overfitting and improve prediction accuracy.

To obtain a better and faster understanding of the extracted features from infected and uninfected images, we also illustrate the feature maps generated by the convolutional layers of the MozzieNet model throughout the training process. Figure 9 represents the feature maps generated by MozzieNet. This feature map is very helpful in understanding how MozzieNet interprets blood cell images. As seen in Figure 9, the filters and kernels in the convolutional layer extract the fine-grained and typical patterns of the infected cell images, which helps the MozzieNet model to improve generalization and achieve excellent results.

On the other hand, the confusion matrix offers detailed insights into the accurate and inaccurate classification of cases, including significant information, such as *trp* (true positive) and *fap* (false positive) cases. We have presented the confusion matrix of the MozzieNet model on the test data in Figure 10. The MozzieNet confusion matrix (Figure 10) shows that the developed model was able to detect 2698 out of 2756 patients infected with malaria and 2634 of 2756 patients who were not infected with malaria. We can see that the fan of the MozzieNet model is very low, which contributes to higher sensitivity values. Figure 11 shows the ROC curve to better understand the performance of MozzieNet. The ROC curve gives the model diagnostic capability to distinguish between infected and uninfected classes. As shown in the figure, the area under the curve (AUC) score obtained by the MozzieNet model is 0.9935.

Since the proposed MozzieNet architecture requires multiple parameters, in order to obtain the best performance, the correct parameters must be used for training. For this, some basic parameters are considered, such as different image sizes, effect of data augmentation, optimizers, and optimal BS. These parameters will be discussed below.

### 4.3.1 | Results comparison with different optimizer functions

The optimizer function is responsible for finding the minimum value of the loss function. Adam Optimizer was selected to perform training on MozzieNet. To evaluate the effectiveness, Adam, SGD, and RMSProp are applied to the MozzieNet model to compare the performance of the optimizers. Table 8 shows the classification results of the various optimizers. The performance results were evaluated on a test set and it can be observed that the Adam optimizer outperforms other competing optimizers. The results presented in Table 6 earlier are, in fact, the outcomes obtained by employing the Adam optimizer.

### 4.3.2 | Effect of data augmentation

The study evaluated the impact of data augmentation on the performance of the MozzieNet model, comparing it with the same model trained without augmentation. Table 9 compares the performance of the MozzieNet model. We found that adding data augmentation techniques to the training pipeline greatly improved the robustness of MozzieNet. The main reason is that data augmentation can prevent data scarcity. Figure 12 shows a performance comparison of MozzieNet.

### 4.3.3 | Comparison of results with different BSs

The impact of BS on enhancing test accuracy is explored in this experiment, and the results are presented in Table 10, which demonstrates MozzieNet's performance on a test set while being trained with various BS. As can be seen from the table, BS 64 has achieved higher and more stable test performance. Therefore, a BS of 64 was chosen for this work.

### 4.3.4 | Effect of different input image size

The size of the input images is an important hyperparameter that can significantly impact the performance of the MozzieNet model, especially since the images in the dataset have varying sizes. Therefore, in this study, the images were resized to a fixed size before being fed into the model. Smaller images require less computation and time, whereas a larger image requires more computational resources. Table 11 shows the results of MozzieNet performance on images of various sizes. For experimental purposes, we resized the image to three different sizes of the same input image:  $25 \times 25 \times 3$ ,  $50 \times 50 \times 3$ , and  $100 \times 100 \times 3$ . Using the proposed



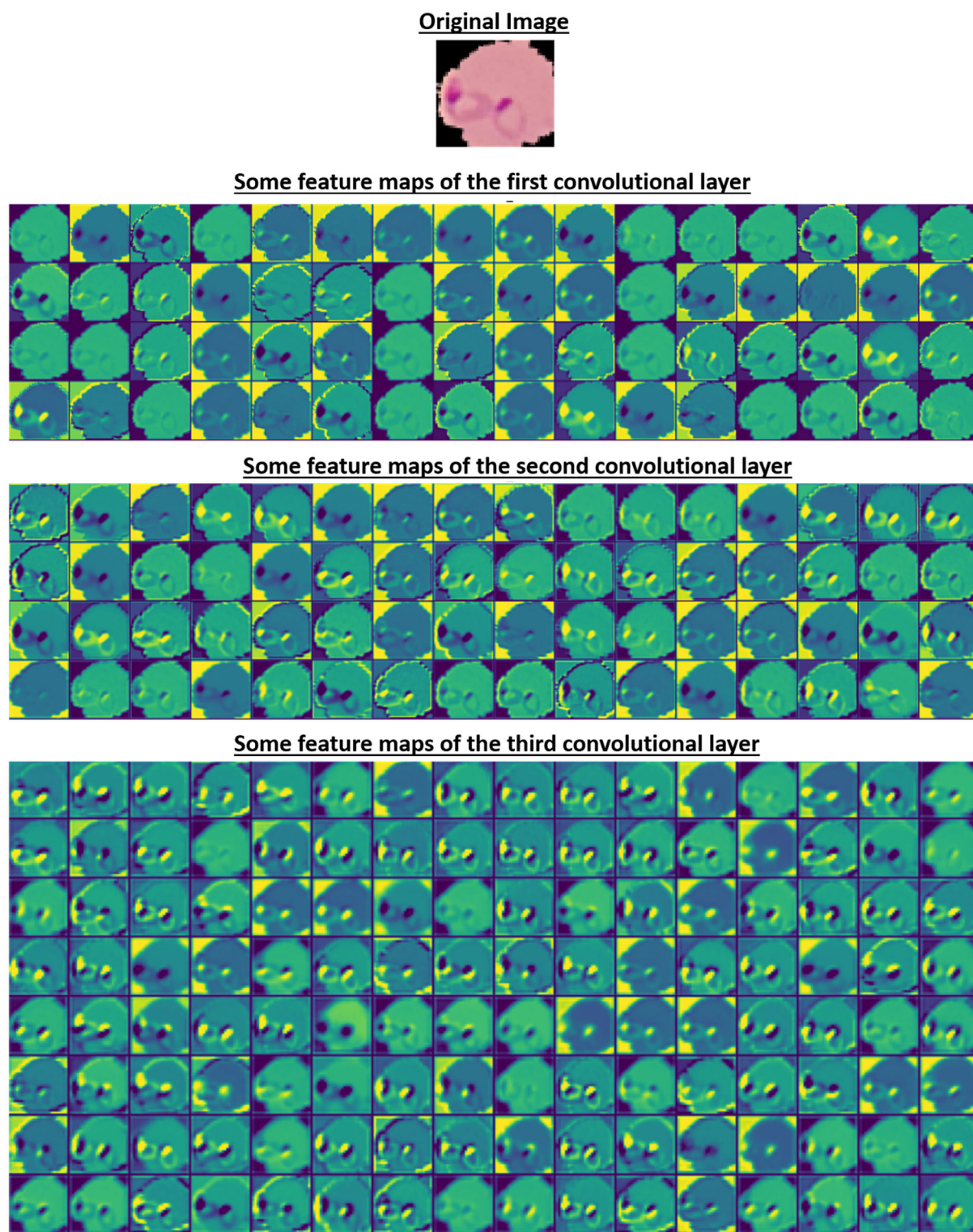


**FIGURE 9** Visualization of the feature map generated by the first three convolution layers of the MozzieNet model.

model, the best result (accuracy = 96.73%) was obtained from slides of  $50 \times 50$  images compared to  $25 \times 25$  (accuracy = 96.46%) and  $100 \times 100$  (accuracy = 95.06%). Since a smaller image size requires less computational costs, for the proposed MozzieNet model, an image size of  $50 \times 50$  pixels was considered.

#### 4.4 | Heatmap visualization

We also studied how the MozzieNet model reached its conclusions to distinguish patients with malaria from normal people. It is important to understand what the model retrieves from the dataset. To achieve this, we used the

Grad-CAM heatmap approach to visualize the important regions that the model emphasizes in the blood cell image. Figure 13 shows a heatmap from the MozzieNet model to

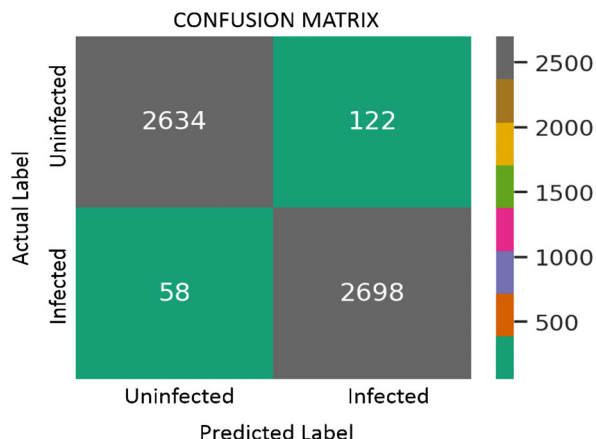


FIGURE 10 Confusion matrix of the MozzieNet model.

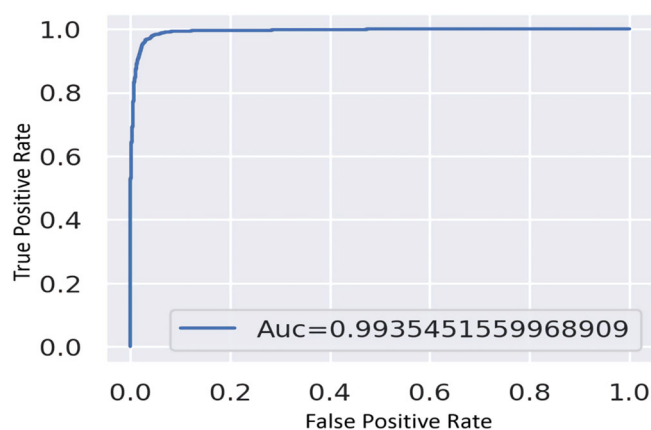


FIGURE 11 ROC curve of the MozzieNet model (AUC score = 0.9935).

TABLE 8 Comparison of MozzieNet classification performance between different optimizers.

Optimizer	ACC (%)	PRE (%)	REC (%)	F1 (%)
Adam	<b>96.73</b>	<b>95.67</b>	<b>97.90</b>	<b>96.77</b>
SGD	94.83	94.78	94.88	94.83
RMSProp	95.64	93.14	98.54	95.76

Note: The bold values indicates the highest values.

TABLE 9 Performance comparison of MozzieNet.

	ACC (%)	PRE (%)	REC (%)
Performance with augmentation	<b>96.73</b>	<b>95.67</b>	<b>97.90</b>
Performance without augmentation	95.30	93.66	97.16

Note: The bold values indicates the highest values.

the suspicious region for the examples of infected samples. These heatmaps show that our model focuses most on abnormal areas while ignoring normal areas, as shown in the infected example. The jet color map is used for heatmaps. Red highlights the activation area related to the predicted category, blue represents unextracted features, and blue and green represent less extracted features.

#### 4.5 | Deployment of MozzieNet model on mobile platform

Mobile phones have become an integral part of our daily lives, and we have developed a streamlined and flexible mobile app to utilize this technology for malaria detection. Our proof-of-concept app, based on MozzieNet, uses cell images to perform simple and rapid detection of malaria parasites. To reduce the model size, we have utilized Google's TensorFlow Lite to convert the model into a .tflite format that is only 7 MB in size. Once deployed on the mobile device, the app loads cell images from the gallery or via a camera and passes them through the model for potential malaria detection. The deployed model provides prediction results after analysis. Figure 14 displays the graphical interface of the real-time malaria detection mobile app.

#### 4.6 | Comparison with pre-trained CNN models

We compared the performance of the MozzieNet model with pre-trained models on the malaria test set. The authors in Reference 15 used five different pre-trained models and applied transfer learning technique to classify blood cells. To enable a fair comparison, we report in Table 12 the results achieved by the MozzieNet model alongside those obtained by the models proposed by Reference 15 for malaria detection using the same dataset. Performance metrics considered for comparisons are accuracy, sensitivity, MCC, F1 score, specificity, and AUC. Although they achieved impressive results, the main problem with the transfer learning model required high computational power and time. We noticed that the MozzieNet model shows better performance than the models presented in Reference 15.



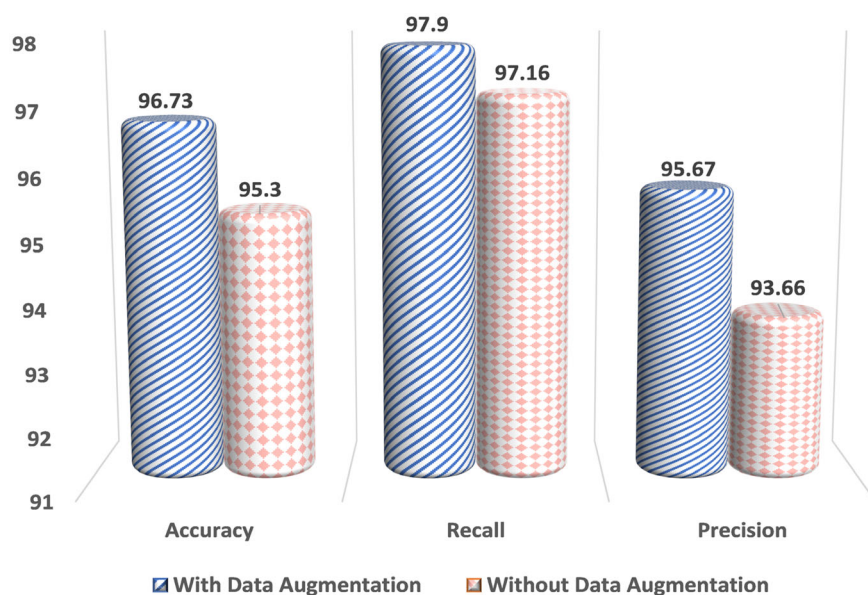


FIGURE 12 Effect of with and without data augmentation on MozzieNet.

Batch size	ACC (%)	PRE (%)	REC (%)	F1 (%)	MCC (%)
16	96.57	95.27	98.04	96.61	93.18
32	95.97	94.02	98.18	96.05	92.03
64	<b>96.73</b>	<b>95.67</b>	<b>97.90</b>	<b>96.77</b>	<b>93.49</b>
128	94.19	90.41	98.87	94.45	88.77

TABLE 10 Performance comparison for different batch sizes.

Note: The bold values indicates the highest values.

TABLE 11 The model performance on test set for different input image sizes.

Input image size	ACC (%)	PRE (%)	REC (%)	F1 (%)
25 × 25	96.46	96.48	96.46	96.46
50 × 50	<b>96.73</b>	<b>95.67</b>	<b>97.90</b>	<b>96.77</b>
100 × 100	95.06	95.38	95.06	95.05

Note: The bold values indicates the highest values.

#### 4.7 | Performance comparison of MozzieNet with the existing techniques

We compared the accuracy of our MozzieNet model with the results of recently published papers on the same problem. Table 13 summarizes the accuracy comparison between our proposed method and existing malaria parasite classification techniques. The table shows that MozzieNet demonstrates the highest performance than other existing schemes. Falcon CNN classifier proposed by Reference 25 achieved 95.20% accuracy. Bibin et al.<sup>26</sup> did not show good performance when compared to the proposed model. K Thom-as et al.<sup>27</sup> achieved an accuracy of 95.70% but showed a lower recall value compared to the proposed model.<sup>16</sup> proposed the model and showed slightly better results in terms of accuracy and F1 score,

but showed very low recall and MCC, which is a very important metric for binary classification. Masud et al.<sup>17</sup> designed a CLR-triangular2 model and achieved better accuracy, but showed low AUC and recall value than our proposed MozzieNet model. Sensitivity is an essential indicator of the accuracy of the model for identifying infected individuals. According to the previous discussion, our MozzieNet model is very specific, has high sensitivity and MCC values, and shows great performance over existing methods.

## 5 | DISCUSSION

In the broader context of the literature on malaria detection, our study introduces the MozzieNet model as a

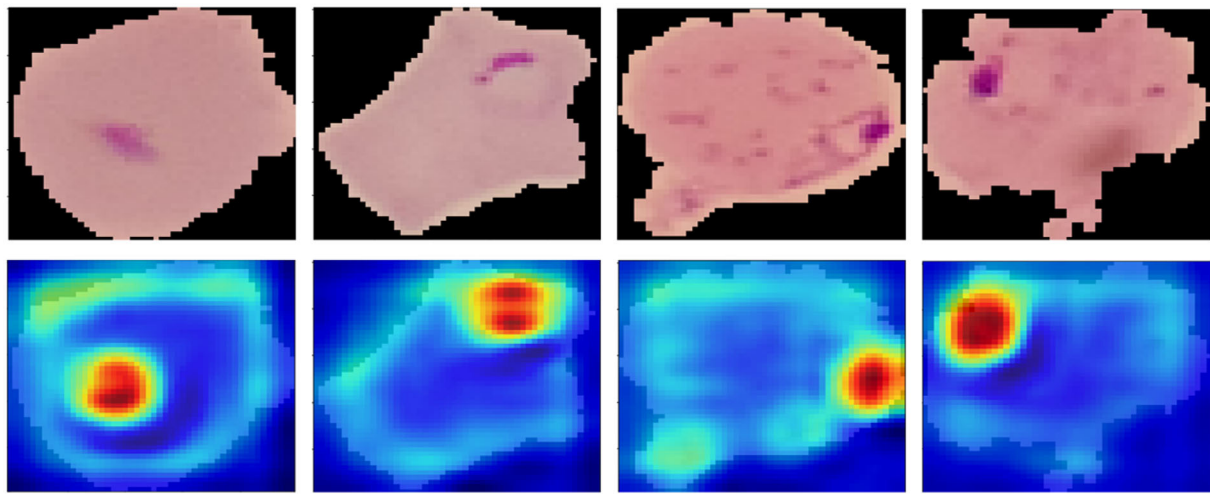


**FIGURE 13** Illustration displaying the original blood smear image (top row) alongside the Grad-CAM activation map (bottom row) of malaria infection.

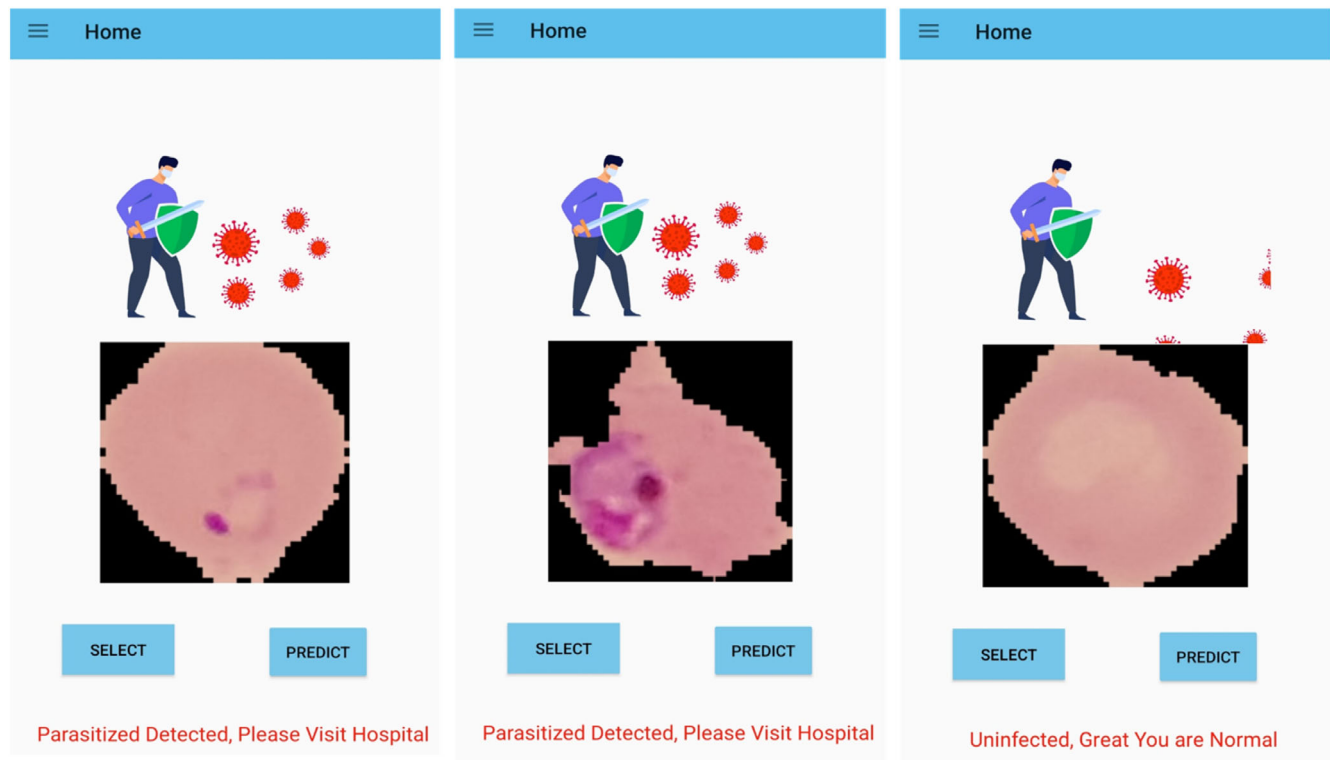


**FIGURE 14** Our app's user interface incorporates MozzieNet model for malaria screening.

novel approach to accurately classify blood smear microscopic images as healthy or infected with malaria. The manual identification of malaria-infected cells is time-consuming and prone to human error, leading to inaccurate reports, particularly in large-scale screening with limited resources. To address this challenge, we have leveraged the power of CNNs to automate the identification process and provide a more efficient and accurate solution for malaria diagnosis. The results of

our study demonstrate the effectiveness of the MozzieNet model in malaria detection. We achieved a classification accuracy of 96.73%, a recall rate of 97.90%, precision of 95.67%, AUC of 99.35%, and F1 score of 96.77% in distinguishing between healthy and infected blood smear images. These findings highlight the capability of MozzieNet to accurately identifying malaria parasites and making it a promising tool for rapid and reliable malaria diagnosis.

**TABLE 12** Performance comparison of MozzieNet with pre-trained models.

Model	ACC (%)	REC (%)	SPEC (%)	MCC (%)	AUC (%)	F1 (%)
AlexNet	93.70	94.00	93.30	87.20	98.10	93.70
VGG-16	94.50	93.90	95.10	88.70	98.10	94.50
ResNet-50	95.70	94.50	96.90	91.20	99.00	95.70
Xception	89.00	93.10	83.50	77.20	94.80	89.50
DenseNet-121	93.10	94.20	92.60	89.40	97.60	93.10
Proposed MozzieNet	<b>96.73</b>	<b>97.90</b>	<b>95.57</b>	<b>93.49</b>	<b>99.35</b>	<b>96.77</b>

Note: The bold values indicates the highest values.

**TABLE 13** Performance comparison of the proposed MozzieNet model with existing methods.

Authors	Model	ACC (%)	REC	SPEC	MCC	AUC	F1
Banerjee et al. <sup>25</sup>	Falcon CNN	95.20	-	-	-	-	-
Bibin et al. <sup>26</sup>	Deep Belief Network	96.30	97.60%	95.92%	-	-	89.66%
K Thomas et al. <sup>27</sup>	Adaptive median filter, Segmentation	95.70	94.50%	96.90%	91.20%	99.00%	95.70%
Gopakumar et al. <sup>16</sup>	Custom CNN	97.70	97.10%	-	73.05%	-	97.70%
Masud et al. <sup>17</sup>	CLR-triangular2	97.30	97.00%	-	94.17%	97.04%	97.00%
Rajaraman et al. <sup>15</sup>	Custom CNN	94.00	93.10%	95.10%	88.80%	97.90%	94.10%
Quan et al. <sup>28</sup>	ADCN	97.47	97.86%	97.07%	-	-	97.50%
Kumar et al. <sup>29</sup>	MosquitoNet	96.60	97.60%	95.80%	93.30%	99.00%	96.70%
Fatima et al. <sup>30</sup>	CAD	91.80	88.60%	95.00%	-	-	91.53%
Proposed method	<b>MozzieNet</b>	<b>96.73</b>	<b>97.90%</b>	<b>95.57%</b>	<b>93.49%</b>	<b>99.35%</b>	<b>96.77%</b>

Note: The bold values indicates the highest values.

What sets our study apart is the optimization of the MozzieNet model's hyperparameters, which include adjusting image sizes, implementing data augmentation techniques, selecting appropriate optimizers, and determining the optimal BS. This optimization process improves the model's robustness and generalization ability, allowing it to perform well across different datasets and enhance its applicability in real-world scenarios. Additionally, we have incorporated techniques such as batch normalization, dropout, and LeakyReLU activation to mitigate overfitting problems commonly encountered in DL models. By addressing these limitations, we have enhanced the MozzieNet model's ability to classify blood smear images accurately and reliably, reducing the risk of false negatives and false positives.

One of the significant contributions of our study is the application of Grad-CAM analysis to provide interpretability and visualize the regions within blood cell images that are critical for accurate predictions. This technique enables medical professionals to gain insights into the areas infected with malaria parasites, enhancing their understanding of the model's decision-making

process and facilitating more informed clinical decision-making.

While our study demonstrates promising results, it is essential to acknowledge the limitations. We utilized the open-source NIH malaria dataset, which may introduce biases and limitations in terms of dataset size and diversity. Further validation on larger and more diverse datasets would strengthen the generalizability of the MozzieNet model and provide more comprehensive insights into its performance across different populations and settings.

Furthermore, although we compared the performance of MozzieNet with pre-trained models commonly used in malaria detection, additional comparative studies with other state-of-the-art methods would provide a more comprehensive evaluation of its effectiveness. Exploring the performance of the model on different datasets and in real-world clinical settings would further validate its practical utility and reliability.

In conclusion, our study addresses the broader context of malaria detection by introducing the MozzieNet model as a novel and efficient approach. By optimizing

hyperparameters, mitigating overfitting, and enhancing interpretability, we have filled gaps and addressed limitations in existing methods. The impressive results achieved by the MozzieNet model demonstrate its potential for rapid and reliable malaria diagnosis. However, further research is needed to validate the model's performance on diverse datasets, compare it with other methods, and assess its applicability in real-world clinical settings. By continually improving and refining the MozzieNet model, we can contribute to the field of malaria diagnosis and ultimately aid in preventing the spread of this life-threatening disease.

## 6 | CONCLUSION

Malaria is a contagious and life-threatening disease worldwide, so a quick and accurate diagnosis of malaria is essential. With the emergence of robust CNN models, medical imaging has become an increasingly popular field of research. Our study aims to contribute to this area by proposing a novel approach to diagnose malaria using blood smear images, which we call MozzieNet. Our approach relies on a CNN model that possesses the capability to classify images with remarkable precision. The model is an end-to-end structure that operates fully automatically, without requiring any manual feature extraction. We showed that selecting the hyperparameters appropriately improves the robustness and generalization ability of the MozzieNet model. To improve the interpretability of the proposed model, we applied the Grad-CAM method. The developed model achieved 96.73% accuracy, 99.35% AUC, 97.90% recall, 95.57% specificity, and 96.77% F1 score for classifying blood smear images into healthy and infected images. We also observed that compared with pre-trained models,<sup>15</sup> the MozzieNet model shows better performance in terms of different evaluation metrics. The performance of the MozzieNet model is superior to existing approaches for classifying blood smear images to assist in screening for malaria disease. We hope that the proposed MozzieNet model will be useful in real-time applications for faster and more efficient screening of malaria-infected patients. In future work, potential areas of focus include expanding the dataset for improved generalizability, exploring advanced techniques such as attention mechanisms, and conducting field validation studies to evaluate the model's performance in real-world clinical settings.

## ACKNOWLEDGMENTS

The authors would like to take this opportunity to thank the Central South University, China, for facilitating the laboratory to carry out this research.

## CONFLICT OF INTEREST STATEMENT

The authors declare no conflicts of interest.

## DATA AVAILABILITY STATEMENT

Data sharing is not applicable to this article as no new data were created or analyzed in this study.

## ORCID

Sohaib Asif  <https://orcid.org/0000-0003-0526-3910>

## REFERENCES

1. World Health Organization. World Malaria Report 2015: 2016.
2. Cox FE. History of the discovery of the malaria parasites and their vectors. *Parasit Vectors*. 2010;3:1-9.
3. Behrens N, Nadjim B. Malaria: an update for physicians. *Infect Dis Clin North Am*. 2012;26:243-259.
4. Masanja IM, McMorrow ML, Maganga MB, et al. Quality assurance of malaria rapid diagnostic tests used for routine patient care in rural Tanzania: microscopy versus real-time polymerase chain reaction. *Malar J*. 2015;14:1-7.
5. Murray CK, Gasser RA Jr, Magill AJ, Miller RS. Update on rapid diagnostic testing for malaria. *Clin Microbiol Rev*. 2008; 21:97-110.
6. Gollin D, Zimmermann C. Malaria: Disease impacts and long-run income differences. 2007.
7. Fuhad K, Tuba JF, Sarker M, et al. Deep learning based automatic malaria parasite detection from blood smear and its smartphone based application. *Diagnostics*. 2020;10:329.
8. Poostchi M, Silamut K, Maude RJ, Jaeger S, Thoma G. Image analysis and machine learning for detecting malaria. *Transl Res*. 2018;194:36-55.
9. Razzak MI, Naz S, Zaib A. Deep learning for medical image processing: overview, challenges and the future. *Classific BioApps*. 2018;26:323-350.
10. Molina A, Rodellar J, Boldú L, Acevedo A, Alférez S, Merino A. Automatic identification of malaria and other red blood cell inclusions using convolutional neural networks. *Comput Biol Med*. 2021;136:104680.
11. Vijayalakshmi A. Deep learning approach to detect malaria from microscopic images. *Multimed Tools Appl*. 2020;79:15297-15317.
12. Delgado-Ortíz M, Molina A, Alférez S, Rodellar J, Merino A. A deep learning approach for segmentation of red blood cell images and malaria detection. *Entropy*. 2020;22:657.
13. Hung J, Carpenter A. Applying faster R-CNN for object detection on malaria images. Paper presented at: Proceedings of the Proceedings of the IEEE Conference on Computer Vision and Pattern Recognition Workshops, 2017; pp. 56-61.
14. Devi SS, Laskar RH, Sheikh SA. Hybrid classifier based life cycle stages analysis for malaria-infected erythrocyte using thin blood smear images. *Neural Comput Appl*. 2018;29:217-235.
15. Rajaraman S, Antani SK, Poostchi M, et al. Pre-trained convolutional neural networks as feature extractors toward improved malaria parasite detection in thin blood smear images. *PeerJ*. 2018;6:e4568.
16. Gopakumar GP, Swetha M, Sai Siva G, Sai Subrahmanyam GRK. Convolutional neural network-based malaria diagnosis from focus stack of blood smear images acquired using custom-built slide scanner. *J Biophotonics*. 2018;11:e201700003.



17. Masud M, Alhumyani H, Alshamrani SS, et al. Leveraging deep learning techniques for malaria parasite detection using mobile application. *Wirel Commun Mob Comput*. 2020;2020:1-15.
18. Liang Z, Powell A, Ersoy I, et al. CNN-based image analysis for malaria diagnosis. Paper presented at: Proceedings of the 2016 IEEE international conference on bioinformatics and biomedicine (BIBM), 2016; pp. 493–496.
19. Yang F, Poostchi M, Yu H, et al. Deep learning for smartphone-based malaria parasite detection in thick blood smears. *IEEE J Biomed Health Inform*. 2019;24:1427-1438.
20. Kassim YM, Palaniappan K, Yang F, et al. Clustering-based dual deep learning architecture for detecting red blood cells in malaria diagnostic smears. *IEEE J Biomed Health Inform*. 2020; 25:1735-1746.
21. Elter M, Haßlmeyer E, Zerfaß T. Detection of malaria parasites in thick blood films. Paper presented at: Proceedings of the 2011 annual international conference of the IEEE Engineering in Medicine and Biology Society, 2011; pp. 5140–5144.
22. Varma SL, Chavan SS. Detection of malaria parasite based on thick and thin blood smear images using local binary pattern. *Computing, Communication and Signal Processing*. Springer; 2019:967-975.
23. Xu B, Wang N, Chen T, Li M. Empirical evaluation of rectified activations in convolutional network. preprint arXiv: 1505.00853. 2015.
24. Selvaraju RR, Cogswell M, Das A, Vedantam R, Parikh D, Batra D. Grad-cam: Visual explanations from deep networks via gradient-based localization. Paper presented at: Proceedings of the Proceedings of the IEEE International Conference on Computer Vision, 2017. pp. 618–626.
25. Banerjee T, Jain A, Sethuraman SC, Satapathy SC, Karthikeyan S, Jubilson A. Deep convolutional neural network (falcon) and transfer learning-based approach to detect malarial parasite. *Multimed Tools Appl*. 2021;81:1-15.
26. Bibin D, Nair MS, Punitha P. Malaria parasite detection from peripheral blood smear images using deep belief networks. *IEEE Access*. 2017;5:9099-9108.
27. Kanaa Thomas FN, Daniel T, Pierre E, Emmanuel T, Philippe B. Automated diagnosis of malaria in tropical areas using 40X microscopic images of blood smears. *Int J Biometric Bioinform*. 2016;10:12.
28. Quan Q, Wang J, Liu L. An effective convolutional neural network for classifying red blood cells in malaria diseases. *Interdiscip Sci Comput Life Sci*. 2020;12:217–225.
29. Kumar A, Singh SB, Satapathy SC, Rout M. MOSQUITO-NET: a deep learning based CADx system for malaria diagnosis along with model interpretation using GradCam and class activation maps. *Expert Syst*. 2021;39(7):e12695.
30. Fatima T, Farid MS. Automatic detection of *Plasmodium* parasites from microscopic blood images. *J Parasit Dis*. 2020;44:69-78.
31. Baygin N, Aydemir E, Barua PD, et al. Automated mental arithmetic performance detection using quantum pattern-and triangle pooling techniques with EEG signals. *Expert Syst Appl*. 2023;227:120306.
32. Tasci I, Tasci B, Barua PD, et al. Epilepsy detection in 121 patient populations using hypercube pattern from EEG signals. *Inf Fusion*. 2023;96:252-268.
33. Erten M, Tuncer I, Barua PD, et al. Automated urine cell image classification model using chaotic mixer deep feature extraction. *J Digit Imaging*. 2023;36:1-12.
34. Gul Y, Muezzinoglu T, Kilicarslan G, Dogan S, Tuncer T. Application of the deep transfer learning framework for hydatid cyst classification using CT images. *Soft Comput*. 2023;27: 7179-7189.

**How to cite this article:** Asif S, Khan SUR, Zheng X, Zhao M. MozzieNet: A deep learning approach to efficiently detect malaria parasites in blood smear images. *Int J Imaging Syst Technol*. 2024;34(1):e22953. doi:[10.1002/ima.22953](https://doi.org/10.1002/ima.22953)